



# MATHEMATICAL MODELLING OF THE DEVELOPMENT OF MECHANICAL INSTABILITY IN FRACTURING SYSTEMS†

V. A. BUCHIN, S. S. GRIGORYAN and G. A. SHAPOSHNIKOVA

Moscow

(Received 2 July 1996)

The dynamics of processes accompanying a loss of stability in a mechanical system are investigated. The mechanical system is in the form of an elastic rod, stretched by an axial load, with one of its lateral surfaces “glued” to a rigid wall. The “glue” is a low-strength elastic material which is subject to brittle fracture at a certain value of the load acting on it. In a fractured segment, the rod surface slides over the wall surface under the action of a dry friction force which is less than the breaking stress. The high sensitivity of the process of the development of instability to small perturbations which initiate the development of instability is established. The system considered is the simplest model of the zone of contact between lithospheric plates which generate earthquakes. © 1997 Elsevier Science Ltd. All rights reserved.

Ideas [1] on the mechanism by which earthquakes develop associate the quick release of the elastic energy of rocks at the seismic centre with the onset of instability of the mechanical state of the deformation zone during the slow accumulation of this energy at the earthquake “preliminary” stage and with the subsequent fracture process which occurs there with the emission of elastic waves. Unfortunately, the numerous hypotheses which exist at the present time concerning the “action” of the seismic centre have not been refined to provide quantitative mathematical models which would enable one to calculate the details of the process in the deformation zone. A simple mechanical system has been proposed in [2] which simulates the details of the process by which instability develops at the seismic centre. Various features of the development of instability are investigated below using this model.

1. We consider a mechanical structure consisting of an elastic semi-infinite rod which is “glued” at a finite section of its length to a rigid fixed base (Fig. 1). A (compressive or tensile) force is applied to the rod at infinity as a result of which fracture of the “glue” can occur in the zone where the bar is glued to the base. This construction is the simplest model of the so-called Benioff zone where one lithospheric plate (1) moves under a second plate (2) and, in the region where they come into contact (the hatched region), the material binding them fractures with the release of elastic energy (an earthquake occurs).

We will study the problem of the mechanics of this structure. The left-hand end of the rod ( $x = 0$ ) is assumed to be free while a specified force (stress)  $P$  is applied at the right-hand end where  $x = \infty$ . In this case, the system can be in equilibrium.

We will confine ourselves to considering the one-dimensional longitudinal displacements of the rod  $w(t, x)$  and we can write the equation

$$\rho_0 \frac{\partial^2 w}{\partial t^2} = \frac{\partial \sigma}{\partial x} - \frac{\tau}{D}; \quad \tau \neq 0, \quad 0 \leq x \leq L; \quad \tau = 0, \quad x > L \quad (1.1)$$

$$\sigma = E \frac{\partial w}{\partial x} \quad (1.2)$$

for determining these displacements with a certain approximation.

Here  $\rho_0$  is the density of the rod,  $\sigma \equiv \sigma_{xx}$  is a component of the stress tensor in the rod,  $\tau$  is the shear stress in the interlayer (in the “glue”) between the rod and the rigid base and on the boundary of the rod,  $D$  is the rod thickness and  $E$  is Young’s modulus of the rod material.

†*Prikl. Mat. Mekh.* Vol. 60, No. 6, pp. 1039–1045, 1996.

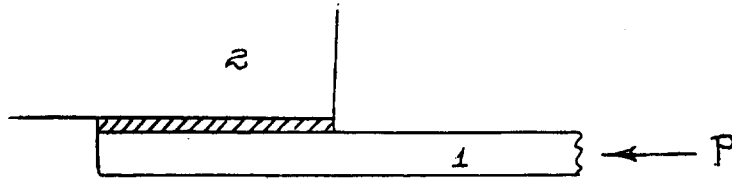


Fig. 1.

It is assumed that the stress  $\tau$  is proportional to the shear strain in the layer  $\gamma = w/h$  ( $h$  is the effective thickness of the layer) for values for  $|\tau|$  which are less than a certain critical value  $\tau_*$  (or for values of  $|\gamma|$  which are less than  $\gamma_*$ ).

$$\tau = G\gamma, \quad 0 \leq |\gamma| < \gamma_*. \quad (1.3)$$

When  $|\tau|$  reaches the value  $\tau_*$ , brittle fracture of the material in the layer occurs. The shear stress  $\tau$  is subsequently determined by the law of dry friction, and it is constant in modulus and equal to  $\tau_{**}$ .

$$\tau = \text{sign}(u)\tau_{**}, \quad \tau_{**} = \text{const}, \quad u = \frac{\partial w}{\partial t} \quad (1.4)$$

An equation in the displacement  $w$  can be obtained from (1.1)–(1.4)

$$\frac{\partial^2 w}{\partial t^2} - a^2 \frac{\partial^2 w}{\partial x^2} = -\frac{\tau}{\rho_0 D}; \quad \tau \neq 0, \quad 0 \leq x \leq L; \quad \tau = 0, \quad x > L; \quad a = \sqrt{\frac{E}{\rho_0}} \quad (1.5)$$

Here  $a$  is the speed of sound in the rod material.

The boundary condition on the left-hand free end of the rod specified in the form

$$\partial w / \partial x = 0, \quad x = 0 \quad (1.6)$$

We will treat the case in which elastic waves are only emitted at the right-hand end of the glued segment of the rod ( $x = L$ ) into the domain  $x > L$ , that is, no perturbations from this domain arrive at the boundary  $x = L$ . This enables us to confine the treatment of the problem solely to the domain  $0 \leq x \leq L$ . In this case, the boundary condition at  $x = L$  can be reduced to the form

$$E \frac{\partial w}{\partial t} + aE \frac{\partial w}{\partial x} = aP, \quad x = L \quad (1.7)$$

We now introduce dimensionless variables using the formulae

$$x = Lx', \quad t = t't_0, \quad t_0 = L/a, \quad w = w_0 w', \quad w_0 = P_0 L / E, \quad \sigma = P_0 \sigma'$$

$$P = P_0 P', \quad \alpha^2 = \frac{L^2 G}{DEh}, \quad P_0^2 = \tau_*^2 \frac{hE}{DG}, \quad q = \frac{\tau_{**}}{\tau_*}$$

2. We will consider the static problem in the case of a static load  $P = P_{st}$ . Its solution  $w = w_0(x)$  satisfies the following system of equations and boundary conditions (henceforth, the prime will be omitted in Section 2)

$$\partial^2 w / \partial x^2 = \alpha^2 \Phi(w), \quad 0 \leq x \leq 1 \quad (2.1)$$

$$\partial w / \partial x = 0, \quad x = 0, \quad \partial w / \partial x = P_{st}, \quad x = 1 \quad (2.2)$$

In the domain where the condition  $0 \leq w < 1/\alpha$  is satisfied, the function  $\Phi(w) = w$  and Eq. (2.1) has the form

$$\partial^2 w / \partial x^2 = \alpha^2 w \tag{2.3}$$

At a place where fracture of the material in the interlayer has occurred, the function  $\Phi(w) = \alpha q \text{sign} P_{st}$  and Eq. (2.1) has the form

$$\partial^2 w / \partial x^2 = \alpha q \text{sign} P_{st} \tag{2.4}$$

The solution of boundary-value problem (2.1), (2.2) is constructed differently for different values of  $P_{st}$ .

If  $|P_{st}| < \text{th } \alpha$ , the interlayer material is not fractured over the whole segment of the rod  $0 \leq x \leq 1$  and, for the solution  $w_0(x)$ , we have

$$w_0(x) = P_{st} \frac{\text{ch } \alpha x}{\alpha \text{sh } \alpha}$$

If  $P_{\max} \geq |P_{st}| \geq \text{th } \alpha$  (the value of  $P_{\max}$  will be determined below), the solution  $w_0(x)$  exists but the material of the interlayer is fractured in the domain  $x_1 < x \leq 1$ . In this case, the stress  $|\sigma|$  decreases monotonically from  $|\sigma| = 0$  when  $x = 0$  to  $|\sigma| = |P_{st}|$  when  $x = 1$ . When  $0 \leq x < x_1$ , the distribution  $w_0(x)$  is determined by the solution of Eq. (2.3) and, when  $x_1 \leq x \leq 1$ , by the solution of Eq. (2.4). The value of  $x_1$  depends on the magnitude of  $|P_{st}|$  and is determined when solving the problem. When  $x = x_1$ , the stress and strain continuity conditions

$$w_0(x-0) = w_0(x+0) = 1/\alpha, \quad \sigma(x-0) = \sigma(x+0)$$

must be satisfied.

In this case, the solution of boundary-value problem (2.1), (2.2) has the form

$$w = \frac{\text{ch } \alpha x}{\alpha \text{ch } \alpha x_1} \text{sign } P_{st}, \quad 0 \leq x \leq x_1 \tag{2.5}$$

$$w = \left\{ \frac{1}{2} \alpha q (x^2 - x_1^2) + (|P_{st}| - \alpha q)(x - x_1) + \frac{1}{\alpha} \right\} \text{sign } P_{st} \tag{2.6}$$

$$x_1 < x \leq 1$$

The magnitude of  $x_1$  is defined by the equation

$$\text{th } \alpha x_1 + \alpha q (1 - x_1) = |P_{st}| \tag{2.7}$$

An analysis of Eq. (2.7) shows that a maximum value of the load  $|P_{st}| = P_{\max}$  exists and, when this is exceeded, no solution of the boundary-value problem exists. The value of  $x_1 = x_{1m} > 0$  corresponds to the value of  $P_{\max}$ .  $P_{\max}$  and  $x_{1m}$  are defined by the expressions

$$P_{\max} = \text{th } \alpha x_{1m} + \alpha q (1 - x_{1m}) \tag{2.8}$$

$$x_{1m} = \frac{1}{\alpha} \ln \left( \sqrt{\frac{1}{q} + \sqrt{\frac{1}{q} - 1}} + \sqrt{\frac{1}{q} - 1} \right) \tag{2.9}$$

A real root  $x_{1m}$  exists if the inequality  $q < 1$  is satisfied.

The case when the root  $x_{1m}$  lies in the interval  $[0, 1]$  is the most interesting. In this case, the static diagram  $P_{st} - \xi$  ( $\xi = 1 - x_1$ ) has a "stable" branch (where  $dP_{st}/d\xi > 0$ ) in the range  $0 \leq \xi \leq 1 - x_{1m}$  and an unstable branch, that is, a branch with  $dP_{st}/d\xi < 0$ , when  $1 - x_{1m} \leq \xi \leq 1$ .

To estimate the values of the dimensionless parameters  $\alpha$  and  $q$ , which determine the solution of the problem, we shall take the following orders of magnitude:  $E = 3 \times 10^{11} \text{ N/m}^2$ ,  $G = 10^{10} \text{ N/m}^2$ ,  $\tau_* = 6 \times 10^6 \text{ N/m}^2$ ,  $\tau_{**} = 0.5\tau_*$ ,  $\rho_0 = 4 \times 10^3 \text{ kg/m}^3$ ,  $L = 3 \times 10^5 \text{ m}$ ,  $h = 10^3 \text{ m}$  and  $D = 5 \times 10^4 \text{ m}$ . With these values of the parameters, we have  $\alpha = 7.746$  and  $q = 0.5$ . In this case,  $P_{\max} = 4.1394$  and  $x_{1m} = 0.113$ . It is easily seen that, as  $\alpha$  increases, the instability domain contracts. The values of  $P_{st}$  and,

correspondingly,  $P_{\max}$  simultaneously decrease. At a fixed value of  $\alpha$ , a decrease in  $q$  enlarges the instability domain with a simultaneous decrease in the value of  $P_{\max}$ .

3. As has been stated above, the static diagram  $P_{\text{st}} - \xi$  ( $\xi = 1 - x_1$ ) has an unstable branch when  $1 - x_{1m} \leq \xi \leq 1$ . This branch is unattainable under static conditions, and the introduction of small perturbations into the system when  $|P_{\text{st}}| = P_{\max}$  leads to dynamic fracture, that is, to a rapid propagation of the fracture front  $\xi = \xi(t)$  from  $1 - x_{1m}$  to 1 with the emission of an elastic wave into the domain  $x > 1$ . In the case of the stable branch, the introduction of perturbations must not lead to any substantial change in the state of the system.

A program was written for calculating unsteady problems for the system of equations and boundary conditions (1.1)–(1.7) in order to investigate dynamic fracture processes.

When  $P = P_{\max}$ , three types of perturbations were introduced into the system: computational perturbations arising from discretization and perturbations of the form

$$\sigma(0, t) = \sigma_0 e(t); \quad e(t) = 0, \quad t < 0; \quad e(t) = 1, \quad t \geq 0 \tag{3.1}$$

$$\sigma(0, t) = \sigma_0 \sin \omega t / t_0 \tag{3.2}$$

It was found that a dynamic process in which instability is “obtained” actually did occur in all cases. In the case of fracture from computational discretization perturbations, the velocity of motion of the discontinuity at the initial stage of fracture is inversely proportional to the number of subdivisions (it falls when there is a reduction in the magnitude of the perturbations) and the curves become similar to one another at the final stage of fracture.

The relation  $\xi(t/t_0)$  is shown in Fig. 2 for the case of fracture arising from perturbations of the type (3.1) (curve 1) and (3.2) (curve 2,  $\omega = 1$ , and curve 3,  $\omega = 40$ ) for  $a = 7.746$ ,  $q = 0.5$ ,  $\sigma_0 = -5$ ,  $\sigma_0 = -5 \times 10^{-2} P_0$  and a number of subdivisions  $N = 1000$ . In this case, the external perturbations are more than an order of magnitude greater than the computational perturbations and the latter have practically no effect on the fracture process. Three stages can be clearly distinguished in the fracture process: after a brief initial stage, which is determined by the amplitude of the perturbation, a state develops with a velocity of the fracture front that depends on the form of the perturbation which alternates with separation which serves as the final stage of progressively accelerating fracture.

We calculated the relations  $u = u(L, t)$  ( $u_0 = w_0/t_0$ ),  $\sigma = \sigma(L, t)$ . These define the elastic wave  $u = u(x - at)$ ,  $\sigma = \sigma(x - at)$  which is emitted into the domain  $x > L$ , that is, the “earthquake”. Calculations were carried out for  $P = P_{\max}$ ,  $\alpha = 7.746$ ,  $q = 0.5$ . A perturbation in the form of (3.2),  $\sigma_0 = -5 \times 10^{-2} P_0$  was specified at the left-hand end ( $x = 0$ ) for various values of  $\omega$ . Note that, while the velocity  $u$  at the left-hand end, varying harmonically takes values of both signs, the velocity  $u$  at the right-hand end only has positive or zero values.

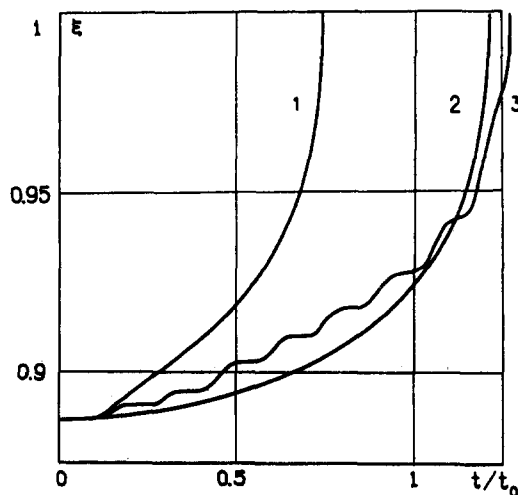


Fig. 2.

In all of the numerical experiments in which a perturbation of the form (3.2) was specified at the left-hand end of the rod, it was found that perturbations of the velocity  $u(x, t)$  of just one sign arose in the fractured domain  $x_1(t) \leq x \leq L$ . The fracture front  $x = x_1$  cuts off the negative part of the harmonic. Furthermore, it is as though the fracture front, on interacting with the wave arriving from the left, reflects part of the positive half-wave to the left.

The distributions  $u(x, t)/u_0$  are shown in Fig. 3 for the instants of time  $t/t_0 = 0.1, 0.4, 1$  and at the instant of fracture  $t = t_f$ . The distributions  $S = (\sigma(x, t) - \sigma(x, 0))/P_0$  are shown in Fig. 4 for the same instants of time. At the instant  $t = 0$ , a perturbation in the form (3.2),  $\sigma_0 = -5 \times 10^{-3}P_0$ ,  $\omega = 40$  is specified at the left-hand end of the bar. Calculations were carried out for  $\alpha = 7.746$ ,  $q = 0.5$ ,  $P = P_{\max}$ . These calculations showed that when  $|\sigma_0|$  is increased by a factor of 10, the maximum and minimum values of  $\sigma$  at the separation stage of the motion of the fracture front are of the same order as when  $\sigma_0 = -5 \times 10^{-3}P_0$ :  $\max S \approx -0.1$ .

There is qualitative agreement between the behaviour of the quantity  $\sigma(x, t) - \sigma(x, 0)$  at the instant of separation and fracture for various values of  $\sigma_0$ . In the interval  $[0, x_{1m}]$  ( $x_{1m} = 0.113$  in the case under consideration), the difference in the stresses increases from practically zero up to the maximum value and then falls to the minimum value. Later, in the interval  $[x_{1m}, 1]$ , this difference increases to zero while oscillating at the same frequency (at the same frequencies  $\omega$ ) but with different amplitudes. The amplitude of these oscillations depends on the value of  $\sigma_0$ .

When a perturbation of the form (3.1) is specified at the initial instant, the fracture front, on interacting with the wave travelling to the right, as in the case when a perturbation in the form (3.2) is specified at the left-hand end, only transmits perturbations which have a positive velocity of motion of the particles  $u$ . It follows from the calculations that the distributions  $u(x, t)$  and  $\sigma(x, t) - \sigma(x, 0)$  for various forms of the perturbations (3.1) and (3.2) only differ slightly from one another in the case of the same  $\sigma_0$  at the final stage before total fracture (separation).

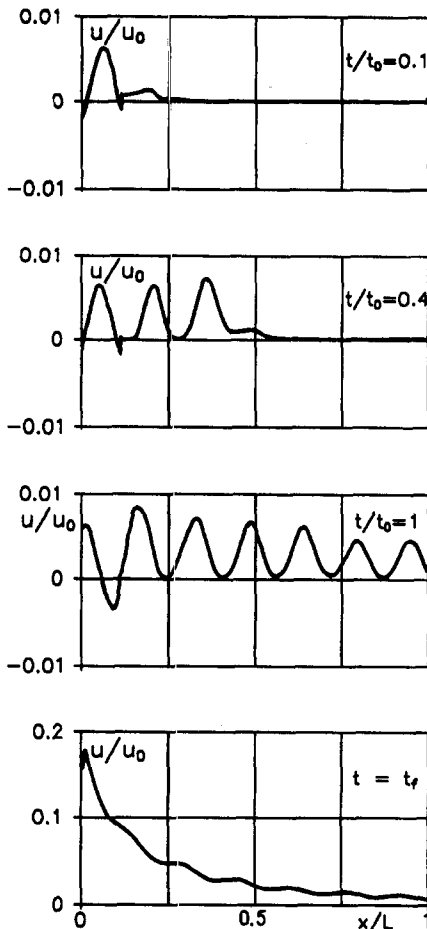


Fig. 3.

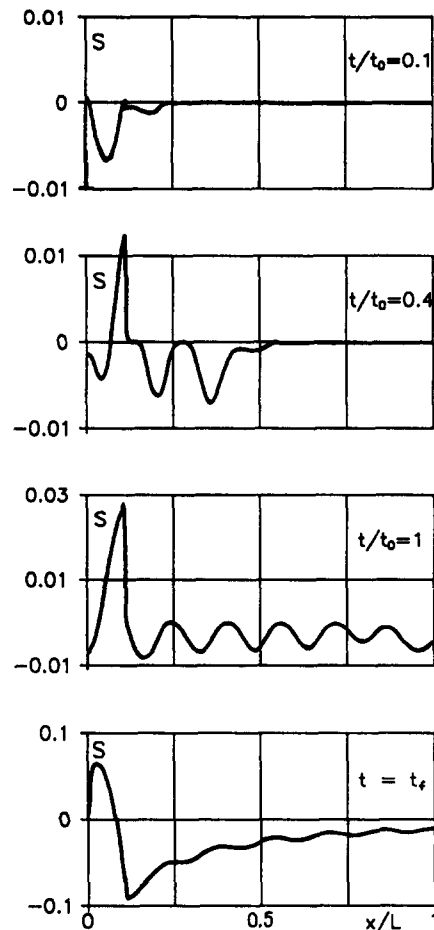


Fig. 4.

This fact, and also the qualitative agreement between the behaviour of the quantity  $\sigma(x, t) - \sigma(x, 0)$  at the instant of separation and fracture for different values of  $\sigma_0$ , stem from the fact that, at the final stage of the motion of the fracture front, the velocity of the motion of the particles of the rod and the change in the stresses are determined by the motion of the fracture front. At the initial stage of fracture, the crack propagation velocity is low and the stresses which arise and the velocity of the particles of the rod are determined by the motion of the perturbation wave and its interaction with the fracture front and the left-hand end of the rod.

Calculations were carried out for a force  $P$ , which was less than  $P_{\max}$  in order to exclude the effect of the motion of the fracture front on the propagation of the perturbation and the interaction of the perturbation with the fracture front. A perturbation in the form (3.1),  $\sigma_0 = -5 \times 10^{-2} P_0$  and  $\sigma_0 = -5 \times 10^{-2} P_0$  was specified at the left-hand end of the rod at the instant of time  $t = 0$  and calculations were carried out with  $\alpha = 7.746$ ,  $q = 0.5$ ,  $P = 4P_0$ . In this case, the coordinate of the fracture front is equal to  $x_1 = 0.2$ .

In the case when  $\sigma_0 > 0$ , we have the following pattern. At the instant of time  $t = 0.2t_0$ , the perturbation incident on the fracture front has negative velocities of the particles and is completely reflected. The reflected wave then interacts with the left-hand end and, at the instant of time  $t = 0.6t_0$ , approaches the fracture front, with the particles having positive velocities. This perturbation is partially reflected and partially travels to the right and, when  $t = 1.4t_0$ , it is emitted into the domain  $x > L$ . In the case when  $\sigma_0 > 0$ , the fracture front is fixed and no wave subsequently appears to the right of the fracture front while a perturbation wave, which is completely reflected both from the fracture front and from the left-hand end of the rod, passes to the left of the fracture zone.

In the case when  $\sigma_0 < 0$ , a perturbation which is incident on the fracture front at the instant of time  $t = 0.2t_0$  has positive particle velocities. It is partially reflected and partially travels into the domain to the right of the fracture front. When  $t = t_0$ , it is emitted into the domain  $x > L$ . When  $\sigma_0 < 0$ , the fracture front is shifted by a small amount into a new equilibrium position and, as in the case when  $\sigma_0 > 0$ , no wave subsequently appears to the right from the fracture front but a wave, which is smaller in amplitude than when  $\sigma_0 > 0$ , travels to the left from the fracture zone and is reflected both from the fracture front and from the left-hand end of the rod.

A numerical investigation was carried out into the dependence of the overall fracture time  $t$  on the amplitude and the form of perturbation introduced.

The dependence of  $t_f/t_0$  on  $\omega$  is shown in Fig. 5. The values of  $\sigma_0 = -5 \times 10^{-3} P_0$ ,  $\alpha = 7.746$ ,  $q = 0.5$  were adopted in the calculations and the dimensionless frequency  $\omega$  was varied from 0 to 80. Curves 1, 2 and 3 correspond to a

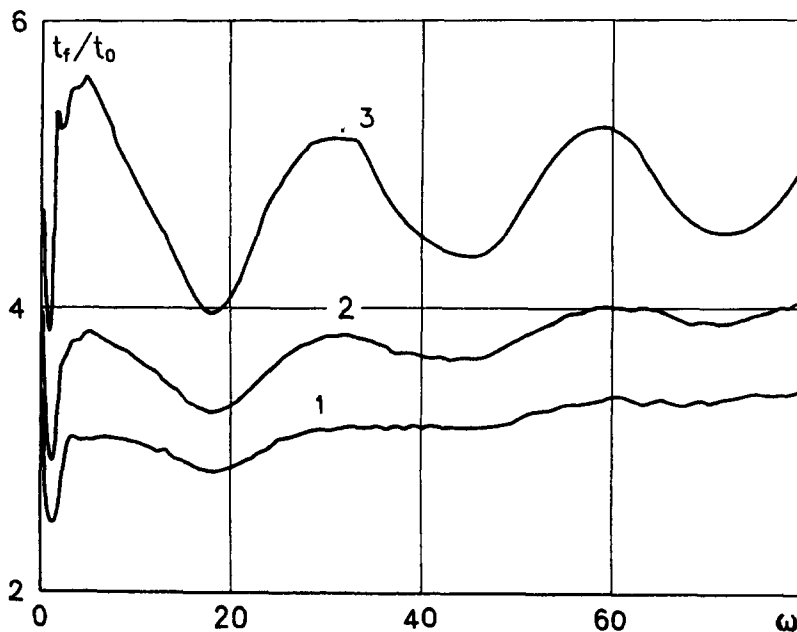


Fig. 5.

number of subdivisions  $N = 1000, 1500, 5000$ . It is clear that the pronounced non-linearity of the problem leads to extremely high sensitivity of the dynamic fracture process, which develops when the critical state is reached, to the nature of the small perturbations which lead to the loss of stability. It is obvious that, for a frequency  $\omega = 0$ , fracture occurs solely due to the action of computational perturbations. In this case, the fracture time depends very much on the number of subdivisions  $N$  and increases from  $t_f/t_0 = 3.7$  when  $N = 1000$  to  $t_f/t_0 = 12$  when  $N = 5000$ . In the case of non-zero values of the frequency  $\omega$ , perturbation from an external action, defined by formula (3.2), interact with the computational perturbations. The results of this interaction is also shown in Fig. 5. It is clear that, regardless of the number of subdivisions, frequencies exist at which the fracture time is a maximum and frequencies at which the fracture time is a minimum. The first global minimum in the fracture time is reached at the frequency  $\omega = 0.9$  and local minima are subsequently reached at frequencies  $\omega \approx 18, \omega = 45, \omega = 72$ . The dependence of the fracture time on the frequency of the perturbation is mainly due to the fact that, as has already been mentioned above, the fracture front does not transmit small perturbations having negative velocities.

The fracture time accompanying harmonic perturbations depends considerably on the sign of the first half-wave, that is, on the sign of  $\sigma_0$ . The curves in Fig. 5 correspond to  $\sigma_0 < 0$ . When  $\sigma_0 > 0$ , the fracture times are greater than when  $\sigma_0 < 0$ .

The fracture time in the case of an external perturbation of the form of (3.1) and  $\sigma_0 > 0$  is substantially greater than when there is no such perturbation (in the case of fracture from computational perturbations).

The above analysis has shown that, even when such a highly simplified model is used, the development of instability in the system after an external load of critical magnitude has been reached is extremely non-trivial, due to the pronounced non-linearity of the mathematical model, which contains mechanisms for a fall off in strength at the instant of local fracture and dry friction in the fractured state. This demonstrates the need for further rigorous investigations into the process of loss of stability at the seismic centre using more complex models for this purpose.

This research was carried out with financial support from the International Science Foundation and the Russian Government (M8M300).

#### REFERENCES

1. GRIGORYAN S. S., The mechanism by which earthquakes occur and the content of the empirical laws of seismology. *Dokl. Akad. Nauk SSSR* 299, 5, 1094–1101, 1988.
2. GRIGORYAN S. S., BUCHIN V. A. and SHAPOSHNIKOVA G. A., Mathematical modelling of the development of instability in fracturing systems. *Dokl. Ross. Akad. Nauk* 349, 4, 533–535, 1996.

Translated by E.L.S.